JOURNAL OF THERMOPHYSICS AND HEAT TRANSFER
Vol. 24, No. 2, April–June 2010

Homogeneous Anisotropic Model for Natural Convection in Nonuniform Layered Porous Cavities

R. L. Marvel III* and F. C. Lai†
University of Oklahoma. Norman, Oklahoma 73019

DOI: 10.2514/1.47050

Steady-state heat transfer by natural convection in a layered porous cavity is examined using a homogeneous anisotropic model. The geometry considered is a two-dimensional square enclosure comprising three or four vertical sublayers with nonuniform thickness and distinct permeability. The cavity is subjected to differential heating from the vertical walls. The results obtained are compared with those reported from a detailed numerical analysis for a wide range of permeability contrast and sublayer thickness ratio. Additionally, the results are compared with the lumped system model that was recently proposed. It has been found that predictions by the homogeneous anisotropic model are reasonably good at a lower Rayleigh number ($Ra_y < 200$). In addition, the predictions improve when the number of sublayers increases, as well as when the sublayer thickness becomes more uniform. Although the homogeneous anisotropic model requires less computational efforts than the full layered model, its predictions only apply to the given effective anisotropy.

Nomenclature

c_p	=	heat capacity, J/kg · K
g	=	gravitational acceleration, m/s^2
H	=	height of cavity, m
h	=	heat transfer coefficient, W/m^2 · K
K	=	permeability, m^2
K_i	=	permeability of sublayer i, m^2
K_x	=	effective permeability in horizontal direction, m^2
K_y	=	effective permeability in vertical direction, m^2
k	=	thermal conductivity, W/m · K
k_i	=	thermal conductivity of sublayer i, W/m · K
k_x	=	thermal conductivity in horizontal direction, W/m · K
k_y	=	thermal conductivity in vertical direction, W/m · K
L	=	width of cavity, m
L_I	=	thickness of sublayer i, m
N	=	number of sublayers
Nu	=	average Nusselt number, hL/k
p	=	pressure, Pa
Ra_y	=	effective Rayleigh number for anisotropic model, $K_1 g\beta(T_h - T_c)L/\alpha\nu$
Ra_1	=	base Rayleigh number, $K_1 g\beta(T_h - T_c)L/\alpha\nu$
T	=	temperature, K
u, v	=	Darcy velocity in the x and y directions, m/s
X, Y	=	dimensionless Cartesian coordinates
x, y	=	Cartesian coordinates, m
α	=	effective thermal diffusivity of porous medium, $\alpha = k/(\rho c_p)_f$, m^2/s
β	=	thermal expansion coefficient, $(-1/\rho)(\partial\rho/\partial T)_p$, K^{-1}
θ	=	dimensionless temperature, $(T - T_c)/(T_h - T_c)$
μ	=	dynamic viscosity of fluid, kg/m · s
ν	=	kinematic viscosity of fluid, m^2/s
ρ	=	fluid density, kg/m^3
ξ	=	permeability anisotropy parameter, K_x/K_y
Ψ	=	dimensionless stream function

Subscripts

c	=	cold wall
f	=	fluid
h	=	hot wall
i	=	index of sublayer (1, 2, ... , N)

Received 5 September 2009; revision received 11 January 2010; accepted for publication 12 January 2010.

*Graduate Research Assistant, School of Aerospace and Mechanical Engineering.

†Professor, School of Aerospace and Mechanical Engineering. Associate Fellow AIAA.

I. Introduction

HEAT transfer in layered porous media has been frequently encountered in engineering applications. Previous studies on layered porous media (either involving pure porous sublayers [1–10] or overlying fluid sublayers [11–15]) have shown that the heat transfer analysis is rather complicated and laborious. As such, a simple method to predict the heat transfer results for layered porous systems is highly desirable. For a layered system involving pure porous sublayers, Leong and Lai [16] have recently proposed a lumped system analysis of heat transfer. They showed that, by properly characterizing a permeability that is representative of the entire layered porous system, the problem is reduced to that of a homogeneous porous medium. They further showed that the effective permeability is defined by the arithmetic mean if the sublayers are oriented parallel to the imposed temperature gradient. On the other hand, the effective permeability based on the harmonic mean is good for sublayers that are perpendicular to the imposed temperature gradient. There is another approach to tackle the problem, which is to use the homogeneous anisotropic model proposed by McKibbin and Tyvand [6,7]. They claimed that, as the number of sublayers increases, the layered porous medium is increasingly better approximated by a homogeneous anisotropic medium. The purpose of this study is to examine the problem considered earlier by the authors [17] using the anisotropic model and compare the results thus obtained with those of the previous study [17] to determine which method would perform better in terms of accuracy, effectiveness, and computational requirement.

II. Formulation and Numerical Method

The geometry considered is a square cavity ($L = H$) consisting of three or four sublayers with nonuniform thickness and distinct permeability (Fig. 1). The permeabilities of these sublayers are alternating among the sublayers (i.e., $K_1 = K_3$ and $K_2 = K_4$). The sublayers are assumed to be saturated with the same fluid. The cavity walls are impermeable. The top and bottom walls are insulated, whereas the vertical walls are differentially heated at constant temperatures T_h and T_c ($T_h > T_c$). In consistence with the homogeneous anisotropic model, the governing equations based on Darcy's law are given by [6,7]:

$$\frac{\partial u}{\partial x}+\frac{\partial v}{\partial y}=0 \tag{1}$$

$$u=-\frac{K_x}{\mu}\frac{\partial p}{\partial x} \tag{2}$$

$$v=-\frac{K_y}{\mu}\left(\frac{\partial p}{\partial y}+\rho g\right) \tag{3}$$

$$\rho c\left(u\frac{\partial T}{\partial x}+v\frac{\partial T}{\partial y}\right)=\left[\frac{\partial}{\partial x}\left(k_x\frac{\partial T}{\partial x}\right)+\frac{\partial}{\partial y}\left(k_y\frac{\partial T}{\partial y}\right)\right] \tag{4}$$

where K_x and K_y are the average permeabilities in the horizontal and vertical direction, respectively. Similarly, k_x and k_y are the average thermal conductivities in the horizontal and vertical directions. For cavities with vertical sublayers, they are given by [6,7]:

$$K_x=\left(\sum_{i=1}^{N}\frac{L_i}{L}\frac{1}{K_i}\right)^{-1};\qquad K_y=\sum_{i=1}^{N}\frac{L_i}{L}K_i \tag{5a}$$

$$k_x=\left(\sum_{i=1}^{N}\frac{L_i}{L}\frac{1}{k_i}\right)^{-1};\qquad k_y=\sum_{i=1}^{N}\frac{L_i}{L}k_i \tag{5b}$$

where subscript i (=1, 2, ... , N) is the index for each sublayer. Because the main focus of the present study is on the effects caused by distinct permeabilities, we tentatively neglect the effect caused by the thermal conductivities for simplicity (i.e., it is assumed $k_x = k_y = k$ for the present study). The corresponding boundary conditions are

$$x=0;\qquad u=0;\qquad T=T_h \tag{6a}$$

$$x=L;\qquad u=0;\qquad T=T_c \tag{6b}$$

$$y=0;\qquad v=0;\qquad \frac{\partial T}{\partial y}=0 \tag{6c}$$

$$y=L;\qquad v=0;\qquad \frac{\partial T}{\partial y}=0 \tag{6d}$$

After invoking Buossinesq's approximation, one can simplify the governing Eqs. (1–4) by introducing the stream function. In the dimensionless form, they are given by

$$\frac{\partial^2\Psi}{\partial X^2}+\frac{1}{\xi}\frac{\partial^2\Psi}{\partial Y^2}=-Ra_y\frac{\partial\theta}{\partial X} \tag{7}$$

$$\frac{\partial\Psi}{\partial Y}\frac{\partial\theta}{\partial X}-\frac{\partial\Psi}{\partial X}\frac{\partial\theta}{\partial Y}=\frac{\partial^2\theta}{\partial X^2}=\frac{\partial^2\theta}{\partial Y^2} \tag{8}$$

where ξ is the effective anisotropy of the layered system defined by McKibbin and Tyvand [6,7], which is given next:

$$\xi=\frac{K_x}{K_y}=\frac{\left(\sum_{i=1}^{N}\frac{L_i}{L}\frac{1}{K_i}\right)^{-1}}{\sum_{i=1}^{N}\frac{L_i}{L}K_i} \tag{9}$$

For a porous cavity with three sublayers, the previous expression is reduced to

$$\xi=\frac{K_1/K_2}{\{2(L_1/L)(K_1/K_2)+[1-2(L_1/L)]\}\{2(L_1/L)+[1-2(L_1/L)](K_1/K_2)\}} \tag{10a}$$

and for four sublayers, it is given by

$$\xi=\frac{K_1/K_2}{4\{(L_1/L)(K_1/K_2)+[(1/2)-(L_1/L)]\}\{(L_1/L)+[(1/2)-(L_1/L)](K_1/K_2)]\}} \tag{10b}$$

An inspection of the effective anisotropy defined previously reveals that the homogeneous anisotropic model treats those layered porous cavities as equivalent if their permeability ratios are reciprocal of one another (e.g., $K_1/K_2 = 0.01$ and $K_1/K_2 = 100$). Neither does the homogeneous anisotropic model make a distinction between the sublayer thickness ratios defined by L_1/L or L_2/L for cavities with an even number of sublayers (e.g., layered porous cavities with $L_1/L = 1/16$ and $L_1/L = 7/16$ are treated as equivalent).

The dimensionless boundary conditions are given next:

$$X=0;\qquad \Psi=0;\qquad \theta=1 \tag{11a}$$

$$X=1;\qquad \Psi=0;\qquad \theta=0 \tag{11b}$$

$$Y=0;\qquad \Psi=0;\qquad \frac{\partial\theta}{\partial Y}=0 \tag{11c}$$

$$Y=1;\qquad \Psi=0;\qquad \frac{\partial\theta}{\partial Y}=0 \tag{11d}$$

For comparison with the results obtained by the lumped system approach, the relation between the effective Rayleigh number for the present study and the base Rayleigh number of the previous study [17] is given by

$$Ra_y=Ra_1\frac{K_y}{K_1} \tag{12}$$

The finite difference method was used to solve the governing equations, along with the boundary conditions. The governing equations and the boundary conditions were discretized using a central difference (except for the convective terms, which were discretized by the upwind scheme). For the present study, various sublayer thicknesses have been considered ($L_1/L = 1/13, 2/13, 3/13, 4/13, 5/13$, and $6/13$ for the case of three sublayers and $L_1/L = 1/16, 1/8, 3/16, 5/16, 3/8$, and $7/16$ for the case of four sublayers). In addition, computations have covered a wide range of the base Rayleigh number ($10 \le Ra_1 \le 1000$) as well as the permeability ratio ($K_1/K_2 = 0.01, 0.1, 1, 10$, and 100). The values of effective anisotropy ξ for the cases considered in the present study are listed in Tables 1 and 2 for cavities with three and four sublayers, respectively. As observed, the value of effective anisotropy decreases when the permeability contrast is larger, as well as when the thickness of the sublayers becomes more uniform.

A uniform grid (1561×1561) with underrelaxation and overrelaxation has been used for the present calculations. The reasons for using this finer grid are twofold; the first reason is that we will be comparing the results with those obtained using a more detailed analysis without resorting to the anisotropic model [17]. For the latter case, a finer grid is required to accommodate the thin sublayers considered. To be consistent, we have used the same grid for both studies. Second, by using such a fine grid, we believe the present results would represent those of the limiting case (i.e., the asymptotic case of zero grid size). Computations have been performed on a 64-bit workstation with 12 GB of RAM and 3.2 GHz dual processors. The required CPU time varies from less than a minute to about 4.5 h, depending on the base Rayleigh number involved. The code developed for the present study has been validated against the results reported in the previous studies for a homogeneous and isotropic

Table 1 Values of effective anisotropy for cavities with three sublayers

L_1/L	$K_1/K_2 = 0.01, 100$	$K_1/K_2 = 0.1, 10$
1/13	0.0727	0.487
2/13	0.0457	0.367
3/13	0.0394	0.332
4/13	0.0413	0.343
5/13	0.0544	0.410
6/13	0.1260	0.635

Table 2 Values of effective anisotropy for cavities with four sublayers

L_1/L	$K_1/K_2 = 0.01, 100$	$K_1/K_2 = 0.1, 10$
1/16, 7/16	0.0853	0.530
1/8, 3/8	0.0516	0.397
3/16, 5/16	0.0417	0.345

porous cavity by setting the value of effective anisotropy ξ to unity. The agreement is found to be excellent and is documented in [18].

Among the results obtained, heat transfer results are of the greatest interest, and they are expressed in terms of Nusselt numbers. The overall Nusselt numbers on the two vertical walls are defined next, respectively [16]:

$$Nu_h = -\int_0^1 \left.\frac{\partial\theta}{\partial X}\right|_{X=0} \mathrm{d}Y \tag{13a}$$

$$Nu_c = -\int_0^1 \left.\frac{\partial\theta}{\partial X}\right|_{X=1} \mathrm{d}Y \tag{13b}$$

It is clear from the previous definitions that the overall Nusselt number represents the total dimensionless heat flux from the vertical wall. An overall energy balance, which is defined next, has been performed in each calculation to further evaluate the accuracy of the results obtained. For the present study, the results are satisfied within 1%:

$$\Delta Nu = \frac{Nu_h - Nu_c}{Nu_h} \tag{14}$$

III. Results and Discussion

A. Cavities with Three Sublayers

The flow and temperature fields in a porous cavity with three sublayers are presented in Figs. 2 and 3, respectively, for various permeability ratios, sublayer thickness ratios, and base Rayleigh numbers. Figure 2a shows the streamline contours for the case of $K_1/K_2 = 0.01$ and 100 (recall that the homogeneous anisotropic model treats these two cases as equivalent). Unlike the results obtained for an actual layered cavity [9,16,17], streamlines for the present case are smooth and do not have kinks at the location of interface. The strength of convection, as indicated by the number of streamlines, reduces when the sublayer thickness becomes more uniform (in other words, as the value of effective anisotropy decreases). As the Rayleigh number increases, the spacing between the streamlines becomes closer in the region near the vertical wall, indicating that the vertical velocity component does increase with the strength of thermal buoyancy. But, there is no change in the velocity at the layer interfaces, as was noticed in the previous studies [9,16,17]. Also, the core of the convective cell remains centered in the cavity instead of moving toward the corner of the cavity. The shape of the convective cell is squashed vertically up to Rayleigh number of 100 but takes on a bow-tie shape thereafter, something not present in the actual layered case. The major difference between the present results and those of the previous studies [9,16,17] is the absence of localized convection in the cavity. In the actual layered case, convection may be confined to the more permeable sublayer. However, using the present model, convection always takes place in the global scale. Based on the classification of flow regimes proposed by Prasad and Kulacki [19], one can conclude from the observation of isotherm contours in Fig. 2b that the flowfield is in the conduction regime up until $Ra_1 = 100$, whereas asymptotic flow regime is apparent for $Ra_1 \geq 500$. No completely horizontal stratification of the isotherms is observed from Fig. 2b, and the isotherms do not become isolated from the top of the cavity, as in the layered cavity. Although the flowfields predicted by the present model do not resemble those of the actual layered cavity, the isotherms (Fig. 2b) are in better agreement for Rayleigh numbers up to 50 when $K_1/K_2 = 100$ and for Rayleigh numbers up to 10 when $K_1/K_2 = 0.01$.

Figure 3 represents the flow and temperature fields for cavities with a permeability ratio of $K_1/K_2 = 0.1$ and 10. Once again, the distribution of the streamlines in Fig. 3a is fairly smooth when compared with those of the actual layered cases with the same permeability ratios [17]. The core of the convective cell remains in the center of the cavity, whereas that of the actual layered system exhibits very different behavior, depending on the permeability ratio. From the previous results [17], they show that, for cavities with a permeability ratio greater than unity, the core of the convective cell moves toward the bottom corner of the heated wall when the Rayleigh number increases. On the other hand, for cavities with a permeability ratio less than unity, an increase in the Rayleigh number causes the core of the convective cell to move toward the top corner of the cooled wall. Again, there is no sudden change in the vertical velocity near the interfaces, as was noted for the actual layered case. However, one does observe a considerable increase in the strength of convective flow as compared with the cases of $K_1/K_2 = 0.01$ and 100 (Fig. 2a) due to an increase in the value of effective anisotropy for the present cases. This observation can also be verified from the isotherm contours presented in Fig. 3b, in which one can clearly observe the transition of the heat transfer mode from conduction to convection. Thermal stratification in the core region at a higher Rayleigh number (e.g., $Ra_1 = 1000$) is also clearly observed, particularly for $L_1/L = 6/13$ which has a maximum value of ξ (Table 1).

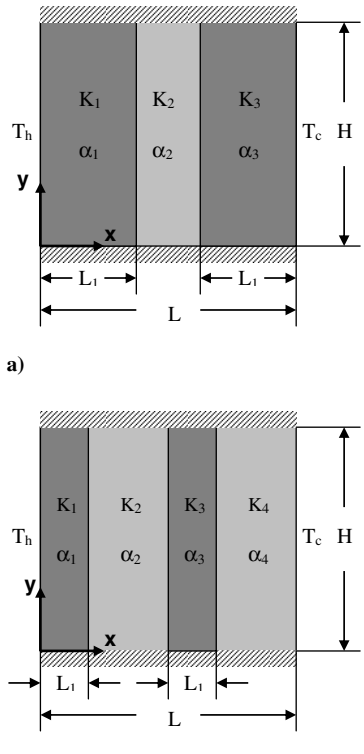

Fig. 1 Layered porous cavities subject to differential heating from two vertical walls: a) three sublayers and b) four sublayers.

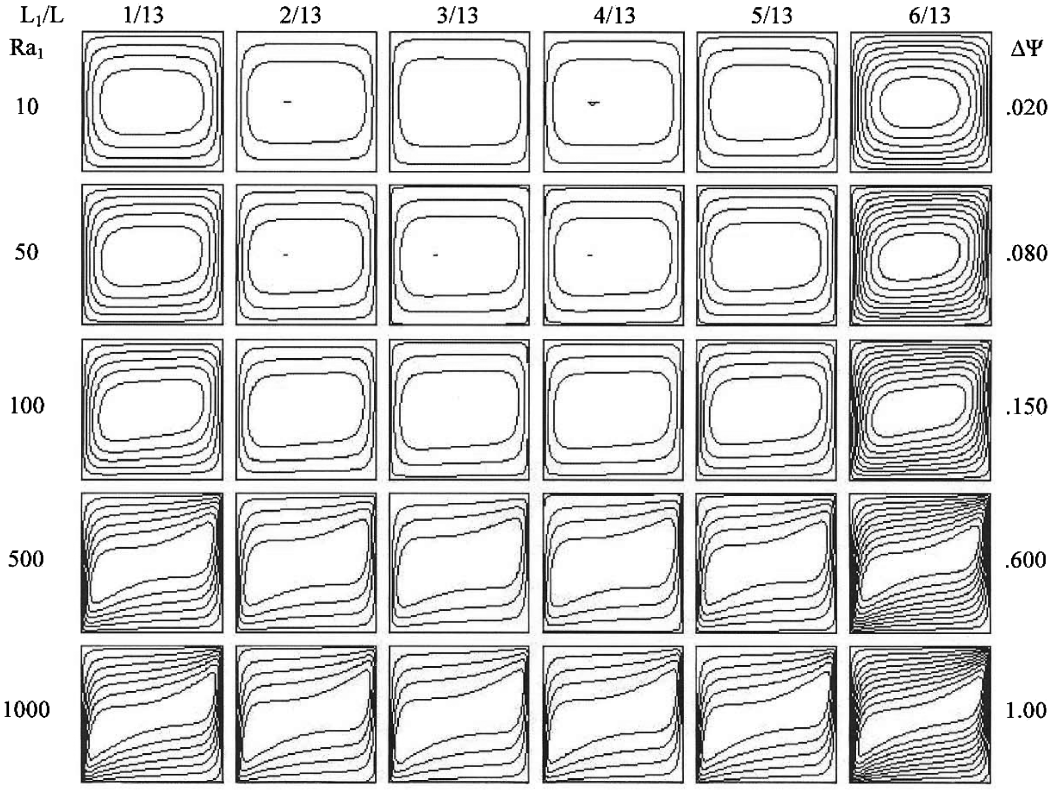

a)

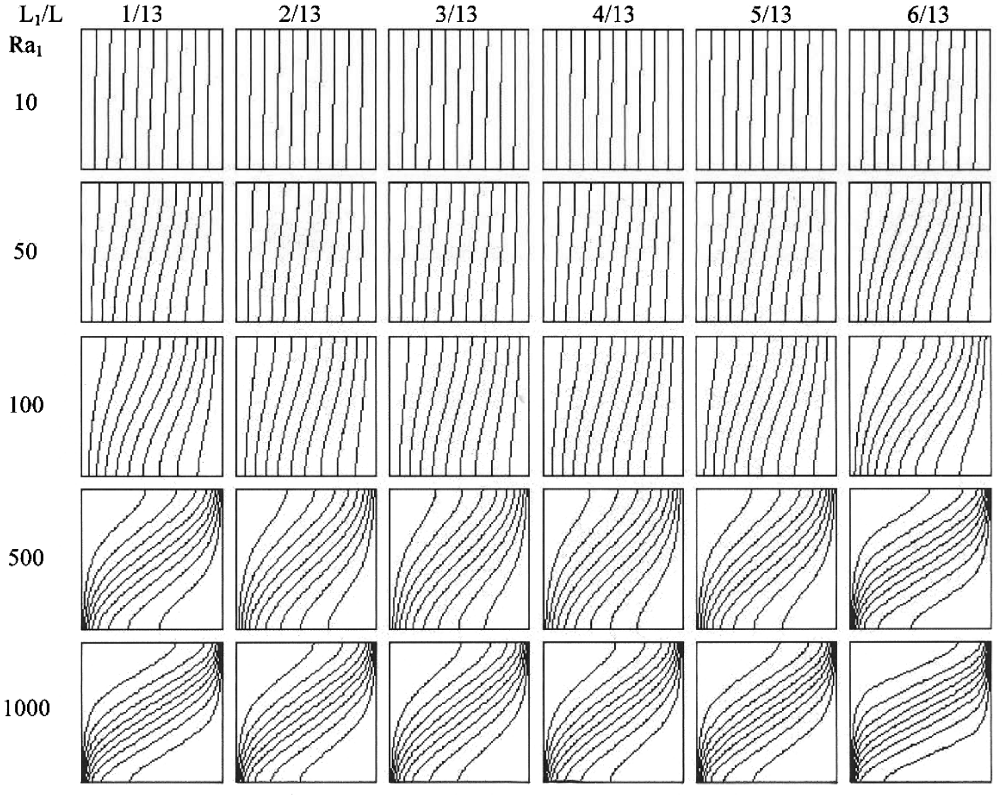

b)

Fig. 2 Flow and temperature fields in a layered porous cavity with three sublayers ($K_1/K_2 = 0.01$ and 100): a) stream function plot ($\Delta\Psi$ as indicated) and b) temperature distribution ($\Delta\theta = 0.1$).

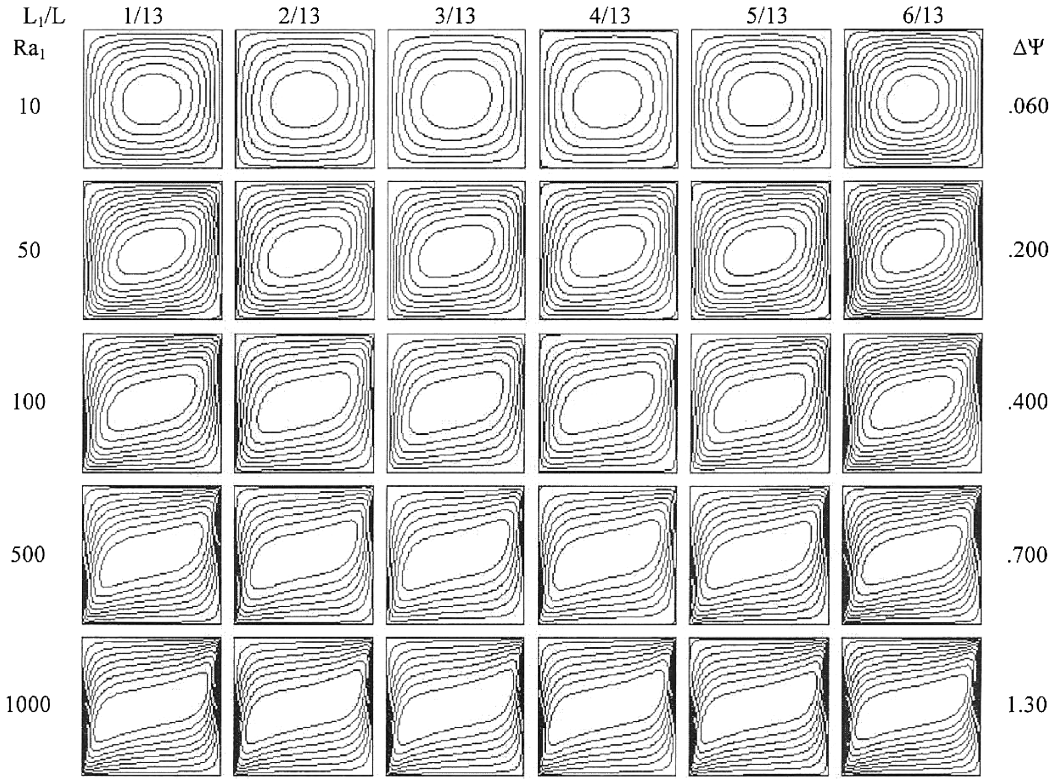

a)

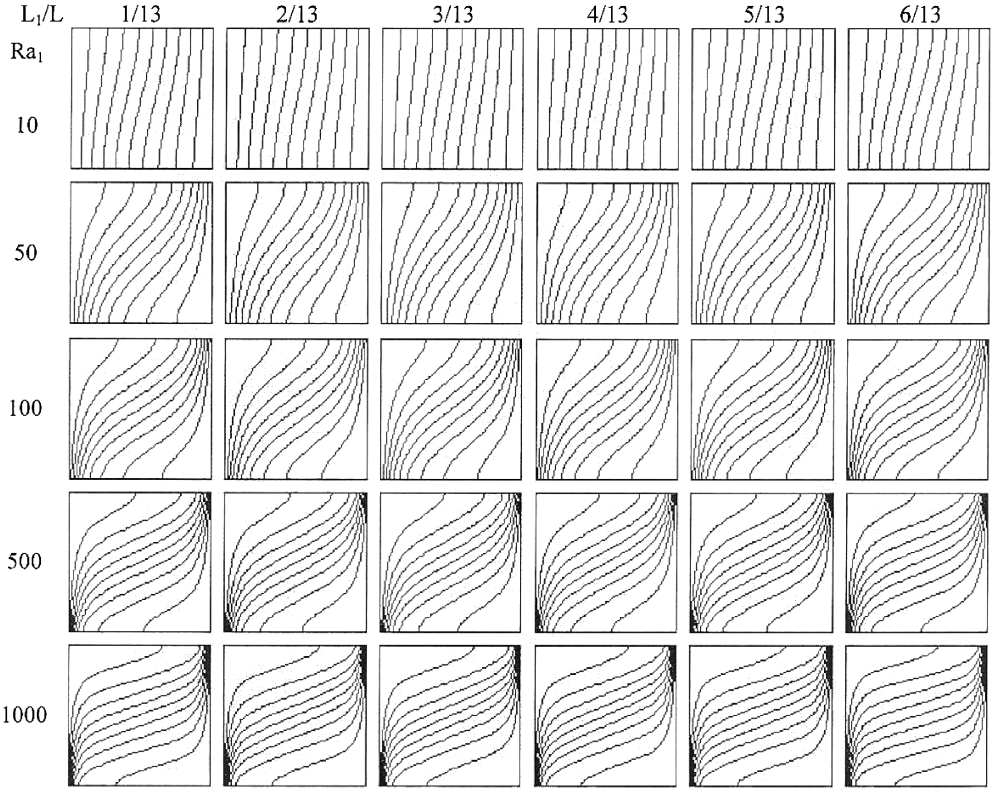

b)

Fig. 3 Flow and temperature fields in a layered porous cavity with three sublayers ($K_1/K_2 = 0.1$ and 10): a) stream function plot ($\Delta\Psi$ as indicated) and b) temperature distribution ($\Delta\theta = 0.1$).

B. Cavities with Four Sublayers

The flow and temperature fields in a porous cavity with four sublayers are shown in Figs. 4 and 5, respectively, for various permeability ratios, sublayer thickness ratios, and base Rayleigh numbers. Figure 4a shows the streamline contours for the cases of $K_1/K_2 = 0.01$ and 100 (again, recall that the homogeneous anisotropic model treats these two cases as equivalent). As indicated by the stream function increment, the strength of the convective cell is much smaller than that for a cavity with three sublayers. This is consistent with the previous observation [16,17] that an increase in the number of sublayers reduces the strength of convective flow. Also consistent with the previous case is that the strength of the convective flow increases with the value of the effective anisotropy. As discussed earlier, an increase in the permeability contrast (Fig. 5a), or a more nonuniform sublayer thickness, would result in a larger value of effective anisotropy. From the isotherm contours shown in Figs. 4b and 5b, one observes that the temperature gradient along the vertical wall is smaller for the case of $K_1/K_2 = 0.01$ and 100 than that of $K_1/K_2 = 0.1$ and 10, indicating that convection is weaker for the former case at a given Rayleigh number. Similar to cavities with three sublayers, convection takes place at the global level, and no localized convection is found. As reported from the previous studies for the actual layered case [9,16,17], convection is first initiated in the more permeable sublayers and then penetrates the less permeable sublayers. Clearly, the homogeneous anisotropic model was not able to reveal the actual flow structure and temperature distribution in a layered porous cavity, particularly for Rayleigh numbers greater than 100.

C. Heat Transfer Results

The average heat transfer coefficients (in terms of Nusselt numbers) are presented as a function of an effective Rayleigh number in Figs. 6 and 7 for cavities with three and four sublayers, respectively. For a layered cavity with three sublayers, the results are shown

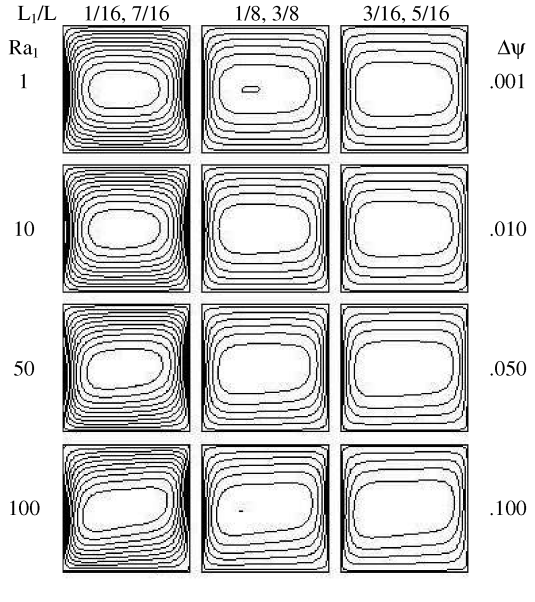

a)

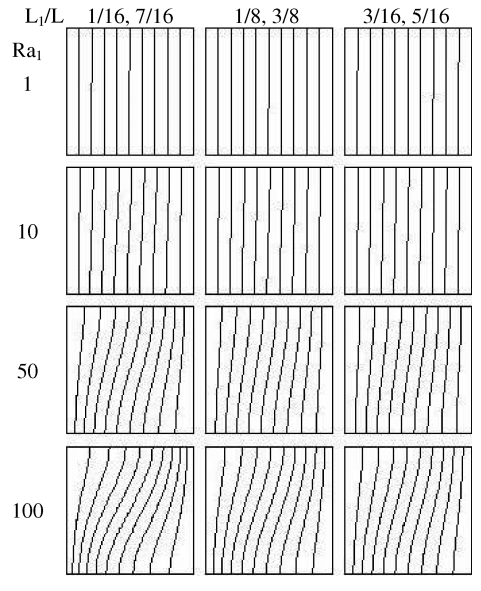

b)

Fig. 4 Flow and temperature fields in a layered porous cavity with four sublayers ($K_1/K_2 = 0.01$ and 100): a) stream function plot ($\Delta\Psi$ as indicated) and b) temperature distribution ($\Delta\theta = 0.1$).

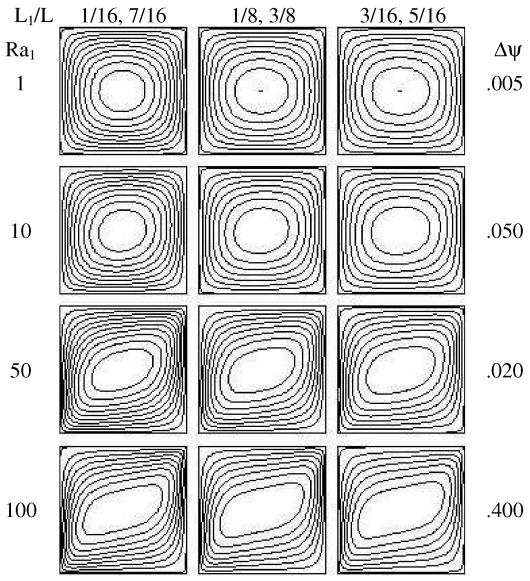

a)

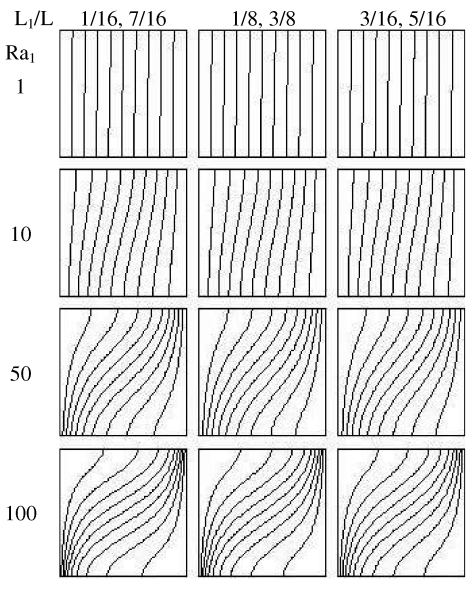

b)

Fig. 5 Flow and temperature fields in a layered porous cavity with four sublayers ($K_1/K_2 = 0.1$ and 10): a) stream function plot ($\Delta\Psi$ as indicated) and b) temperature distribution ($\Delta\theta = 0.1$).

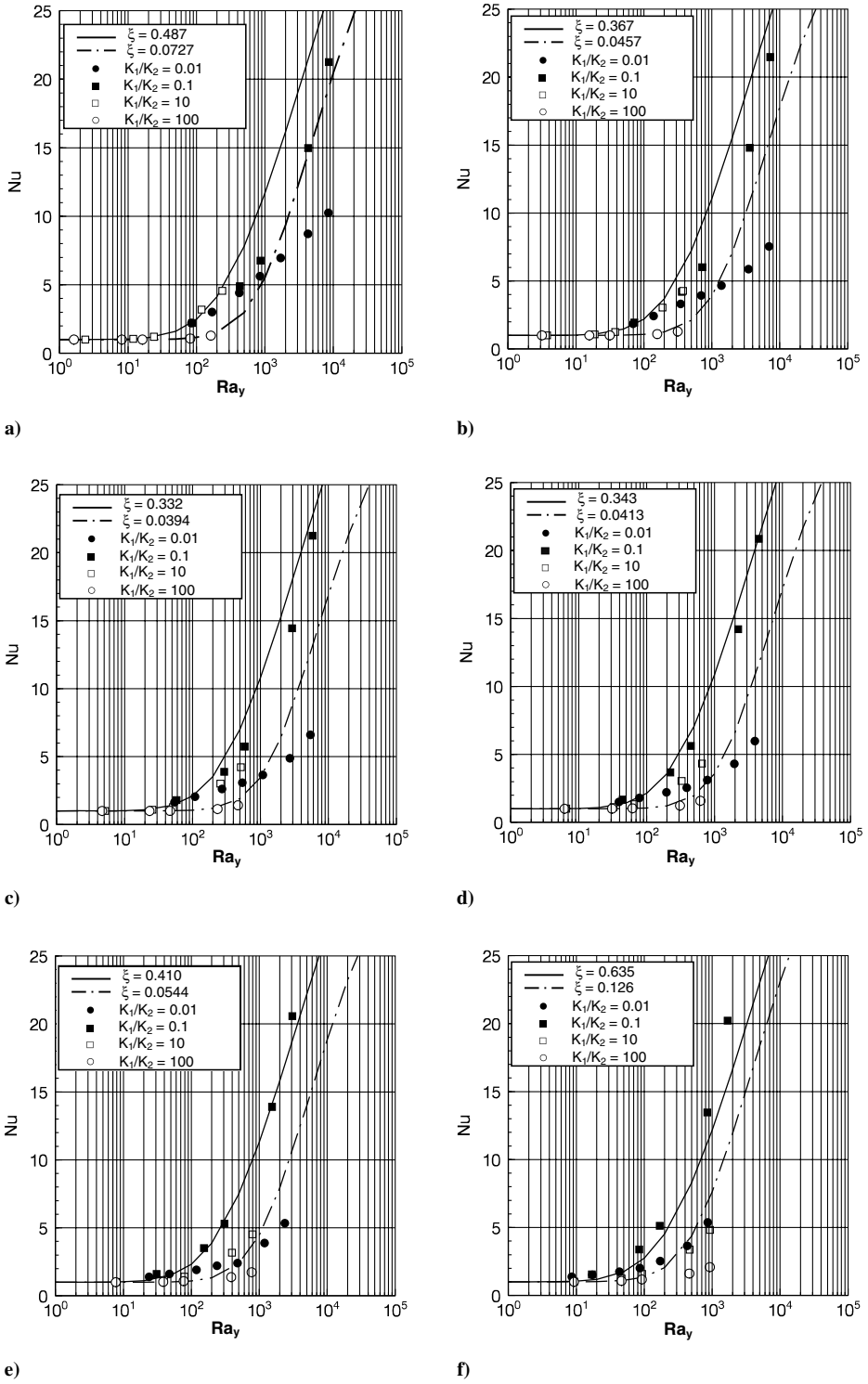

Fig. 6 Heat transfer results for cavities with three sublayers: L_1/L= a) 1/13, b) 2/13, c) 3/13, d) 4/13, e) 5/13, and f) 6/13.

in Figs. 6a–6f for each sublayer thickness ratio considered. In each figure, data obtained from the previous study of actual layered case [17] are plotted with the results predicted by the homogeneous anisotropic model. If the model prediction is good, the curve should pass through the data points with the same value of effective anisotropy. For example, for $L_1/L = 1/13$, the curve of $\xi = 0.487$ should pass through the data points for the cases of $K_1/K_2 = 0.1$ and 10 (Fig. 6a) if the prediction is good. Similarly, the curve of $\xi = 0.0727$ should fit those data points for the cases of $K_1/K_2 = 0.01$ and 100. From Fig. 6, one first observes that, for a given Rayleigh number, the Nusselt number increases with the effective anisotropy ξ. This is consistent with the earlier observation that a cavity with a large value of effective anisotropy has a stronger convective flow, thus leading to a larger heat transfer coefficient. One also observes that a better agreement between the model prediction and the actual data generally can be found at a lower Rayleigh number (e.g. $Ra_y \leq 100$). Although the model prediction may be excellent for some cases at a higher Rayleigh number, this is not generally true for all cases. Specifically, it has been observed that, for the cases of $K_1/K_2 < 1$, the agreement between the model prediction and the actual data is improved as the sublayer thickness ratio increases. But, an opposite trend is observed for the cases of $K_1/K_2 > 1$.

The heat transfer results for a layered cavity with four sublayers are presented in Figs. 7a–7c for each sublayer thickness ratio considered.

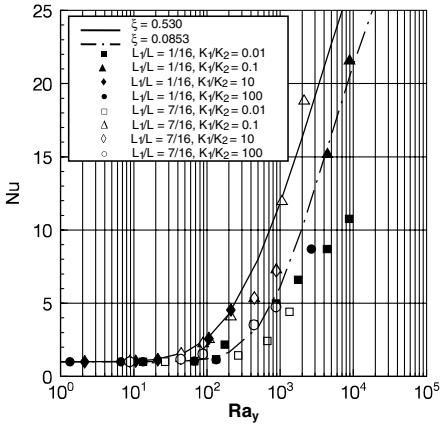

a)

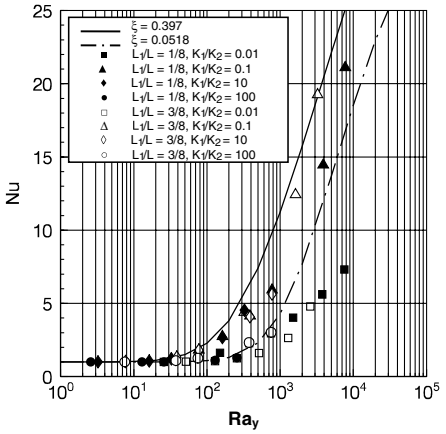

b)

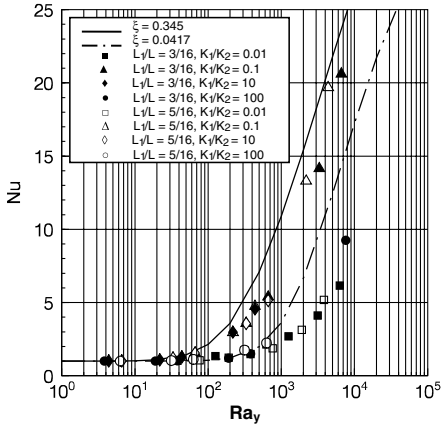

c)

Fig. 7 Heat transfer results for cavities with four sublayers: $L_1/L=$ a) 1/16 and 7/16, b) 1/8 and 3/8, and c) 3/16 and 5/16.

Similar to the results of cavities with three sublayers, one observes that a better agreement between the model prediction and the actual data is found at a lower Rayleigh number. It is observed that the agreement is quite good up to $Ra_y = 200$, which is higher than that for the three-layer case, as it is understood that the homogeneous anisotropic model would produce a better prediction when the number of sublayers increases. It is also interesting to note that data become less scattered when the sublayers are more uniform (i.e., $L_1/L = 3/16$ and $5/16$, Fig. 7c). It also appears that the best agreement exists when the sublayers are more uniform and the permeability contrast is not too large (i.e., $L_1/L = 3/16$ and 5/16 and $K_1/K_2 = 0.1$ and 10, Fig. 7c).

When comparing with the lumped system analysis [17], one notices that both models do not produce perfect prediction of heat transfer results for a layered porous cavity over the entire range of the Rayleigh number. However, their predictions are acceptable for the range of Rayleigh numbers encountered in most practical applications. Especially, the computational requirements for both models are considerably less than that required by the actual layered model; they are very useful when a quick estimate of the heat transfer result is needed. For the homogeneous anisotropic model, the computational requirement is moderate but substantially less than that of the actual layered model. To use this model, one first needs to calculate the value of effective anisotropy for the corresponding layered system and perform numerical calculations for that particular system. The savings in computation is that one does not have to deal with the interface conditions as the actual layered model does. But the drawback is that the results thus obtained cannot be generalized to other systems with different values of effective anisotropy. The lumped system model requires the least effort, because it is based on the results from a homogeneous isotropic cavity, which have already been well documented in the literature. All one needs to do is characterize the effective permeability of the layered system in question, use it to calculate the effective Rayleigh number, and find the corresponding Nusselt number through a proper correlation for homogeneous isotropic cavities.

IV. Conclusions

The present study reexamines the problem of natural convection in a layered porous cavity using a homogeneous anisotropic model. It has been shown that heat transfer results depend on the number of sublayers, the sublayer thickness ratio, and the permeability ratio. These governing parameters can be conveniently grouped into a single parameter called effective anisotropy. For a given Rayleigh number, it has been found that the Nusselt number increases with the effective anisotropy. When comparing the results obtained from the previous study [17] for the actual layered model, one observes that the computational efforts are considerably reduced (the savings in computational time can be as high as tenfold). The agreement between the model prediction and the data of the actual layered case is good at a small Rayleigh number ($Ra_y < 200$) and, with varying degrees of success, at a higher Rayleigh number. The agreement generally improves when the number of sublayers increases or the sublayer thicknesses become more uniform. In comparison with the lumped system model, one finds that the computational effort for the lumped system model is less than that for the homogeneous anisotropic model. In addition, heat transfer results from the layered porous cavity are better fit and follow the same trend of the lumped system model. As such, the lumped system model is considered more accurate and effective than the homogeneous anisotropic model.

References

[1] Masuoka, T., Katsuhara, T., Nakazono, Y., and Isozaki, S., "Onset of Convection and Flow Patterns in a Porous Layer of Two Different Media," *Heat Transfer - Japanese Research*, Vol. 7, No. 1, 1978, pp. 39–52.

[2] McKibbin, R., and O'Sullivan, M. J., "Onset of Convection in a Layered Porous Medium Heated from Below," *Journal of Fluid Mechanics*, Vol. 96, No. 2, Jan. 1980, pp. 375–393. doi:10.1017/S0022112080002170

[3] Rees, D. A. S., and Riley, D. S., "The Three-Dimensional Stability of Finite-Amplitude Convection in a Layered Porous Medium Heated from Below," *Journal of Fluid Mechanics*, Vol. 211, Feb. 1990, pp. 437–461. doi:10.1017/S0022112090001641

[4] Donaldson, I. G., "Temperature Gradients in the Upper Layers of the Earth's Crust Due to Convective Water Flows," *Journal of Geophysical Research*, Vol. 67, No. 9, 1962, pp. 3449–3459. doi:10.1029/JZ067i009p03449

[5] Rana, R., Horne, R. N., and Cheng, P., "Natural Convection in a Multi-Layered Geothermal Reservoir," *Journal of Heat Transfer*, Vol. 101,

No. 3, 1979, pp. 411–416.

[6] McKibbin, R., and Tyvand, P. A., "Anisotropic Modelling of Thermal Convection in Multilayered Porous Media," *Journal of Fluid Mechanics*, Vol. 118, May 1982, pp. 315–339. doi:10.1017/S0022112082001104

[7] McKibbin, R., and Tyvand, P. A., "Thermal Convection in a Porous Medium Composed of Alternating Thick and Thin Layers," *International Journal of Heat and Mass Transfer*, Vol. 26, No. 5, 1983, pp. 761–780. doi:10.1016/0017-9310(83)90027-3

[8] Poulikakos, D., and Bejan, A., "Natural Convection in Vertically and Horizontally Layered Porous Media Heated from the Side," *International Journal of Heat and Mass Transfer*, Vol. 26, No. 12, 1983, pp. 1805–1814.

[9] Lai, F. C., and Kulacki, F. A., "Natural Convection Across a Vertical Layered Porous Cavity," *International Journal of Heat and Mass Transfer*, Vol. 31, No. 6, 1988, pp. 1247–1260. doi:10.1016/0017-9310(88)90067-1

[10] Nield, D. A., Kuznetsov, A. V. K., and Simmons, C. T., "The Effects of Strong Heterogeneity on the Onset of Convection in a Porous Medium: Non-Periodic Global Variation," *Transport in Porous Media*, Vol. 77, No. 2, 2009, pp. 169–186. doi:10.1007/s11242-008-9297-6

[11] Nishimura, T., Takumi, T., Shiraishi, M., Kawamura, Y., and Ozoe, H., "Numerical Analysis of Natural Convection in a Rectangular Enclosure Horizontally Divided into Fluid and Porous Regions," *International Journal of Heat and Mass Transfer*, Vol. 29, No. 6, 1986, pp. 889–898. doi:10.1016/0017-9310(86)90184-5

[12] Beckermann, C., Ramadhyani, S., and Viskanta, R., "Natural Convection Flow and Heat Transfer Between a Fluid Layer and a Porous Layer Inside a Rectangular Enclosure," *Journal of Heat Transfer*, Vol. 109, No. 2, 1987, pp. 363–370. doi:10.1115/1.3248089

[13] Ochoa-Tapia, J. A., and Whitaker, S., "Heat Transfer at the Boundary Between a Porous Medium and a Homogeneous Fluid," *International Journal of Heat and Mass Transfer*, Vol. 40, No. 11, 1997, pp. 2691–2707. doi:10.1016/S0017-9310(96)00250-5

[14] Chen, X. B., Yu, P., Winoto, S. H., and Low, H. T., "A Numerical Method for Forced Convection in Porous and Homogeneous Fluid Domains Coupled at Interface by Stress Jump," *International Journal for Numerical Methods in Fluids*, Vol. 56, No. 9, 2008, pp. 1705–1729. doi:10.1002/fld.1575

[15] Chen, X. B., Yu, P., Sui, Y., Winoto, S. H., and Low, H. T., "Natural Convection in a Cavity Filled with Porous Layers on the Top and Bottom Walls," *Transport in Porous Media*, Vol. 78, No. 2, 2009, pp. 259–276. doi:10.1007/s11242-008-9300-2

[16] Leong, J. C., and Lai, F. C., "Effective Permeability of a Layered Porous Cavity," *Journal of Heat Transfer*, Vol. 123, No. 3, 2001, pp. 512–519. doi:10.1115/1.1351164

[17] Marvel, R. L., and Lai, F. C., "Natural Convection from a Layered Porous Cavity with Sublayers of Nonuniform Thickness: A Lumped System Analysis," Vol. 132, No. 3, *Journal of Heat Transfer*, 2010, pp. 1–6. doi:10.1115/1.3213527

[18] Marvel, R. L., "Comparison of Two Predictive Methods for Natural Convection in Layered Porous Cavities with Non-Uniform Sublayer Thickness," M.S. Thesis, Mechanical Engineering, Univ. of Oklahoma, Norman, OK, 2008.

[19] Prasad, V., and Kulacki, F. A., "Convective Heat Transfer in a Rectangular Porous Cavity: Effect of Aspect Ratio on Flow Structure and Heat Transfer," *Journal of Heat Transfer*, Vol. 106, No. 1, 1984, pp. 158–165. doi:10.1115/1.3246629